



## OPEN ACCESS

## EDITED BY

Vladimir F. Niculescu,  
Other, Germany

## REVIEWED BY

Dharmendra Kumar Yadav,  
Gachon University, Republic of Korea  
Olga V. Anatskaya,  
Russian Academy of Sciences (RAS), Russia  
Jiann-Ruey Hong,  
National Cheng Kung University, Taiwan

## \*CORRESPONDENCE

Mahmoud E. S. Soliman,  
✉ soliman@ukzn.ac.za

RECEIVED 26 September 2024

ACCEPTED 11 December 2024

PUBLISHED 07 January 2025

## CITATION

Elamin G, Zhang Z, Dwarka D, Kasumbwe K, Mellem J, Mkhwanazi NP, Madlala P and Soliman MES (2025) Integrative genomic analyses combined with molecular dynamics simulations reveal the impact of deleterious mutations of Bcl-2 gene on the apoptotic machinery and implications in carcinogenesis. *Front. Genet.* 15:1502152. doi: 10.3389/fgene.2024.1502152

## COPYRIGHT

© 2025 Elamin, Zhang, Dwarka, Kasumbwe, Mellem, Mkhwanazi, Madlala and Soliman. This is an open-access article distributed under the terms of the [Creative Commons Attribution License \(CC BY\)](https://creativecommons.org/licenses/by/4.0/). The use, distribution or reproduction in other forums is permitted, provided the original author(s) and the copyright owner(s) are credited and that the original publication in this journal is cited, in accordance with accepted academic practice. No use, distribution or reproduction is permitted which does not comply with these terms.

# Integrative genomic analyses combined with molecular dynamics simulations reveal the impact of deleterious mutations of Bcl-2 gene on the apoptotic machinery and implications in carcinogenesis

Ghazi Elamin<sup>1,2</sup>, Zhichao Zhang<sup>3</sup>, Depika Dwarka<sup>4</sup>, Kabange Kasumbwe<sup>5</sup>, John Mellem<sup>5</sup>, Nompumelelo P. Mkhwanazi<sup>6</sup>, Paradise Madlala<sup>6,7</sup> and Mahmoud E. S. Soliman<sup>1\*</sup>

<sup>1</sup>Molecular Bio-Computation and Drug Design Laboratory, School of Health Sciences, University of KwaZulu-Natal, Westville Campus, Durban, South Africa, <sup>2</sup>Department of Pharmaceutical Chemistry, College of Pharmacy, Karary University, Khartoum, Sudan, <sup>3</sup>School of Chemistry, Dalian University of Technology, Dalian, Liaoning, China, <sup>4</sup>Ezintsha, Faculty of Health Sciences, University of Witwatersrand, Johannesburg, South Africa, <sup>5</sup>Biotechnology and Food Science, Durban University of Technology, Durban, South Africa, <sup>6</sup>HIV Pathogenesis Programme, School of Laboratory Medicine and Medical Science, The Doris Duke Medical Research Institute, Nelson R. Mandela School of Medicine, University of KwaZulu-Natal, Durban, South Africa, <sup>7</sup>School of Laboratory Medicine and Medical Sciences, University of KwaZulu-Natal, Durban, South Africa

**Objectives:** Unlike other diseases, cancer is not just a genome disease but should broadly be viewed as a disease of the cellular machinery. Therefore, integrative multifaceted approaches are crucial to understanding the complex nature of cancer biology. Bcl-2 (B-cell lymphoma 2), encoded by the human Bcl-2 gene, is a critical anti-apoptotic protein that regulates cell death pathways, primarily by inhibiting apoptosis. It plays a pivotal role in maintaining cellular homeostasis by preventing premature or excessive cell death. Genetic variations and dysregulation of Bcl-2 are particularly significant in cancer, as they disrupt the normal apoptotic machinery, enabling cancer cells to evade programmed cell death. Single nucleotide polymorphisms (SNPs) are considered viable diagnostic and therapeutic biomarkers for various cancers. Therefore, this study explores the association between SNPs in Bcl-2 and the structural, functional, protein-protein interactions (PPIs), drug binding and dynamic characteristics.

**Methods:** Comprehensive cross-validated bioinformatics tools and molecular dynamics (MD) simulations. Multiple sequence, genetic, structural and disease phenotype analyses were applied in this study.

**Results:** Analysis revealed that out of 130 mutations, approximately 8.5% of these mutations were classified as pathogenic. Furthermore, two particular variants, namely, Bcl-2<sup>G101V</sup> and Bcl-2<sup>F104L</sup>, were found to be the most deleterious across all

analyses. Following 500 ns, MD simulations showed that these mutations caused a significant distortion in the protein conformational, protein-protein interactions (PPIs), and drug binding landscape compared to Bcl-2<sup>WT</sup>.

**Conclusion:** Despite being a predictive study, the findings presented in this report would offer a perspective insight for further experimental investigation, rational drug design, and cancer gene therapy.

#### KEYWORDS

Bcl-2, nsSNPs, mutations, genomic analyses, molecular dynamics simulations

## 1 Introduction

The complex nature of cancer biology imposes a major challenge in cancer research and, consequently, the development of effective treatment regimes. The World Health Organization (WHO) estimated that 10 million patients globally died from various forms of cancer in 2020 alone. Many clinical trials do not provide significant success despite significant advances in diagnosis and innovative therapy methods (Karimi et al., 2022). Even though targeted therapy has been a successful approach in treating cancer, heterogeneous cancer still has a variety of clinical profiles and molecular alterations. Certain genetic alterations in cancer targets can make drugs more effective or, more often, cause them to become resistant to treatment (Jin et al., 2019). Drug resistance caused by mutations is a common occurrence in cancer. Thus, the mutation profile of patient malignancies plays a major role in determining the effectiveness of targeted therapy. Accurate molecular and genetic profiling of tumour cells is becoming a crucial step before implementing targeted therapy in patients (Jin et al., 2019).

Apoptosis, a programmed cell death process, is critical for maintaining cellular homeostasis and plays a pivotal role in preventing cancer development by eliminating defective cells. The oncoprotein B-cell lymphoma-2 (Bcl-2) family of proteins, comprising both pro-apoptotic and anti-apoptotic members, regulates the intrinsic pathway of apoptosis by controlling mitochondrial outer membrane permeabilization (MOMP) (Adams and Cory, 2017). Dysregulation of these proteins can lead to apoptosis evasion, a hallmark of cancer, highlighting their importance in oncogenesis and as potential therapeutic targets (Czabotar et al., 2014).

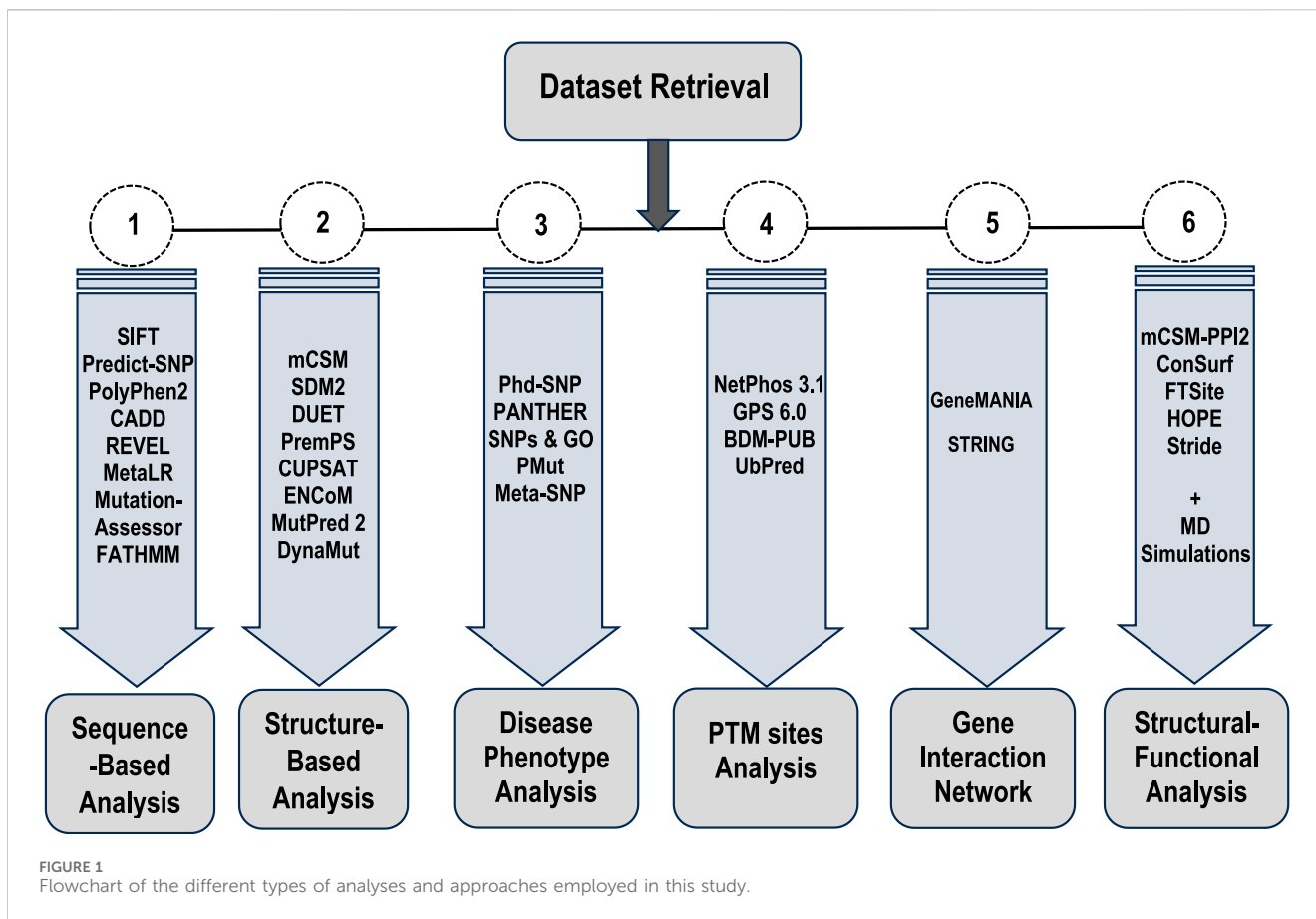
Apoptosis is mediated through two main pathways: the intrinsic (mitochondrial) pathway and the extrinsic (death receptor) pathway. The intrinsic pathway is regulated by the Bcl-2 family, where the balance between anti-apoptotic proteins (such as Bcl-2) and pro-apoptotic proteins (such as Bax and Bak) determines cell survival or death (Youle and Strasser, 2008). The extrinsic pathway, triggered by external signals, activates death receptors leading to caspase activation (Lavrik et al., 2005).

Recent research challenges the traditional view that the Bcl-2 family of proteins directly initiates cancer. Instead, current evidence suggests a more nuanced role where these proteins intervene in processes such as tetraploidization-dependent senescence, contributing indirectly to the cancerous phenotype (Barriuso et al., 2023). Tetraploidization, the process by which cells double their genome and typically undergo senescence to prevent malignant transformation, is intricately regulated by the Bcl-2 family. These proteins are key players in determining cell fate

after tetraploidization, deciding between senescence and further steps leading to aneuploidy, a hallmark of cancer cells (Barriuso et al., 2023). Moreover, the initiation of carcinogenesis is increasingly understood to involve mechanisms that maintain unicellular genome integrity, such as DNA repair pathways and responses to hyperpolyploidy (Niculescu V, 2024; Niculescu V. F., 2024; Niculescu and Niculescu, 2024). These processes are crucial for cellular survival under stress but can also lead to genomic instabilities when dysregulated, setting the stage for cancer development (Chatterjee and Walker, 2017; Conway et al., 2024). The interplay between the Bcl-2 family proteins and these genomic maintenance mechanisms offers a potential explanation for their role in cancer beyond their traditional functions in apoptosis regulation. In light of these insights, the BCL-2 family's influence on cancer appears linked with its impact on cellular responses to genome duplication errors and subsequent genomic instability. This perspective aligns with findings that implicate disrupted apoptosis pathways and aberrant cell survival signals in the broader context of cellular genome management, rather than direct oncogenic transformations.

Recent research has also expanded our understanding of apoptosis, revealing its more nuanced roles beyond the traditional pathway of programmed cell death. Particularly, the phenomenon of anastasis, the process by which cells recover from the brink of apoptosis, has garnered significant attention (Vasileva et al., 2024). Anastasis provides critical insights into cellular resilience and has profound implications for cancer therapy, where the ability of cells to evade death can contribute to treatment resistance (Mohammed et al., 2022). Anastasis not only challenges the finality traditionally associated with apoptosis but also highlights the “dark side” of apoptosis, where apoptotic processes contribute unexpectedly to cancer progression and other diseases (Zaitceva et al., 2021). This aspect of apoptosis, often referred to as its “dark side,” involves mechanisms where sub-lethal apoptotic signaling promotes adaptive capabilities in cells, potentially leading to enhanced metastatic properties and therapeutic resistance (Vasileva et al., 2024). The study of anastasis has revealed that cells can reverse death processes, a capability that was previously unrecognized. This reversal is not merely a return to homeostasis but often results in cells that acquire new properties or heightened survival strategies, which can include resistance to anti-cancer drugs. Understanding the signaling pathways involved in anastasis could open new avenues for cancer treatment, potentially leading to therapies that prevent the reversal of apoptosis in malignant cells (McDonald et al., 2021).

Incorporating the concepts of anastasis and the dark side of apoptosis into the current framework of cancer biology not only



enhances our understanding of cellular death but also underscores the complexity of targeting apoptotic pathways in cancer therapy. These insights emphasize the need for a deeper investigation into the molecular mechanisms that govern these processes to devise more effective therapeutic strategies.

In recent years, Bcl-2 family proteins have been widely recognized for their central role in regulating apoptosis, which is critical in the context of cancer therapy. High Bcl-2 expression in solid tumors has often been associated with enhanced responsiveness to certain anticancer therapies. However, the role of Bcl-2 is not unequivocally beneficial, as the regulation of apoptosis in solid tumors presents both opportunities and challenges in clinical settings (Ichim and Tait, 2016; Kalkavan et al., 2023; Nano and Montell, 2024). While high Bcl-2 expression can render some tumor cells more susceptible to apoptosis induction, it can also contribute to therapy resistance by inhibiting the apoptotic pathways of specific chemotherapeutic agents or targeted therapies (Ichim and Tait, 2016; Kalkavan et al., 2023; Nano and Montell, 2024). These complexities highlight the need to carefully consider the dual role of Bcl-2 and the broader implications of apoptosis regulation in therapeutic strategies. Addressing these challenges requires an integrated understanding of apoptotic and non-apoptotic pathways and their interplay in solid tumors to optimize therapeutic outcomes.

Bcl-2 family proteins control apoptosis and are implicated in various tumour progressions (Rosser et al., 2003; Goff et al., 2013). This gene was the first to promote prolonged cell survival and

growth rather than boost proliferation, demonstrating the importance of inhibiting cell death in tumorigenesis (Cory and Adams, 2002). Bcl-2 inhibits cytochrome c (cyt-c) release from the mitochondria, preventing caspases involved in apoptosis from activating (Yin et al., 1994). Bcl-2 overexpression or aberrant expression has been associated with many cancers' emergence, progression, and relapse (Delbridge et al., 2016; Kitada et al., 2002). Consequently, Bcl-2 activity and protein levels have emerged as essential measures for determining the success or failure of clinical treatment and predicting patient outcomes (Delbridge et al., 2016). The sensitivity of malignant tumor cells to apoptosis can be efficiently boosted by either lowering Bcl-2 protein levels or suppressing Bcl-2 function (Qian et al., 2022). Multidrug resistance (MDR) in cancer cells can be overcome by selectively inhibiting Bcl-2, resulting in cell cycle arrest, senescence, and eventual cell death in response to radiotherapy and chemotherapy (Tang et al., 2020; Wang et al., 2020). Therefore, inhibition of Bcl-2 inactivation has become a highly attractive strategy in the battle against cancer, and BH3 mimetics are the main category of promising therapeutic agents (Perini et al., 2018; Delbridge and Strasser, 2015). BH3 mimetics inhibit Bcl-2 activity by competing with its physiological ligands, BH3 domain-containing pro-apoptotic proteins, at the hydrophobic (binding) groove (Czabotar et al., 2014).

Despite the promising initial clinical effectiveness of BH3 mimetic agents in various cancers, the mutation is a common way cancer cells evade therapies (Roberts et al., 2016;

Stilgenbauer et al., 2018). The most common mutation is a change from glycine to valine at amino acid position 101 (G101V), which substantially decreases Bcl-2 affinity towards the BH3 mimetics agent (Venetoclax) and prevents the drug from displacing pro-apoptotic mediators from Bcl-2 in the cells (Blombery et al., 2019; Blombery et al., 2020). Most human genetic variations are attributable to single nucleotide polymorphisms (SNPs) (Dakal et al., 2017). This genetic variation generated by SNPs in genetic codons influences the translation outcome, resulting in a mutant protein with a different structure and function. Nevertheless, not all SNPs impact protein function and structure; a few are harmful, but many are not (Kucukkal et al., 2015).

Bioinformatics offers enormous array of databases and techniques that are necessary for the analysis, integration, and interpretation of cancer multi-omics data (Jiménez-Santos et al., 2022). It is noteworthy that *in silico* techniques have recently emerged as valuable tool to assess the distinct genomic alterations and transcriptome profiles of tumors, as well as understanding the underlying mechanisms of cancer (Yalcin-Ozkat, 2021; Edelman et al., 2010; Elamin et al., 2024).

The primary goal of this study is to explore the effects of single nucleotide polymorphisms (SNPs) in the Bcl-2 gene on the structural, functional, and dynamic properties of the Bcl-2 protein. The specific objectives are to: identify and classify SNPs in the Bcl-2 gene and assess their pathogenic potential using bioinformatics and validated computational tools; analyze the structural and functional impacts of deleterious Bcl-2 mutations on protein-protein interactions (PPIs) and drug-binding characteristics; and pinpoint key mutations, such as Bcl-2<sup>G101V</sup> and Bcl-2<sup>F104L</sup>, that significantly affect protein behavior, offering valuable insights for cancer diagnostics and therapeutic strategies. By identifying pathogenic SNPs and their effects on Bcl-2, the study enhances understanding of the molecular mechanisms underpinning apoptosis resistance in cancer. Moreover, the study highlights SNPs with diagnostic and therapeutic potential, offering a foundation for the development of biomarkers for cancer diagnosis and prognosis.

To achieve the objectives of this study, a combination of *in silico* methods, bioinformatics approaches, and molecular dynamics simulations was utilized to comprehensively investigate the genomic and proteomic alterations in Bcl-2 (Figure 1) and their potential roles in carcinogenesis. To ensure cross-validation and the reliability of the generated data, multiple bioinformatics algorithms were employed for each type of analysis conducted. Several mutations were examined for their potential contributions to cancer initiation and progression, with their deleterious effects on the structure and function of Bcl-2 thoroughly characterized. Subsequently, the most deleterious mutations, Bcl-2<sup>G101V</sup> and Bcl-2<sup>F104L</sup>, were selected for further dynamic analysis to probe their impact on the protein conformational landscape using molecular dynamics (MD) simulations and post-dynamic analyses.

We believe that the extensive and multifaceted analyses provided in this study will offer a thorough grasp of the effects of deleterious Bcl-2 gene mutations on the apoptotic machinery and their implications for carcinogenesis. Our findings would contribute to the broader discourse on the genetic underpinnings of cancer, illustrating how specific

SNPs can alter key apoptotic regulators such as Bcl-2. This understanding will then inform future directions in drug design and the development of anti-cancer therapeutics.

## 2 Methods

### 2.1 Generation of the datasets

The Bcl-2 FASTA sequence was obtained from UniProt (UniProt ID: P10415) (<https://www.uniprot.org/>) (Bateman et al., 2017). The dbSNP (<https://www.ncbi.nlm.nih.gov/snp/>) and Ensembl (<https://www.ensembl.org/>) databases and an extensive literature search were used to compile the list of mutations (Sherry et al., 2001; Hubbard et al., 2002). Gene synonyms (Bcl-2, PPP1R50) (transcript ID: ENST00000333681.5) of the Bcl-2 protein were selected for this study. Duplicate variants and other redundant data were excluded from the analysis. High-resolution crystal structures of the Bcl-2 protein, both wild-type and mutated (G101V and F104L) (PDB ID:6O0K, 6O0L, and 6O0M), were obtained from the Protein Data Bank (<https://www.rcsb.org/>) (Birkinshaw et al., 2019).

### 2.2 Sequence-based analyses for point mutation

We utilised eight different bioinformatics tools to obtain a reliable cross-validated sequence-based analysis to determine the deleterious effects of residue mutations on the protein. These are, the Sorting Intolerant From Tolerant (SIFT) algorithm (<https://sift.bii.a-star.edu.sg>) which determines the deleterious effects of residue mutations on proteins (Kumar et al., 2009); Polymorphism Phenotyping 2 (PolyPhen-2) (<http://genetics.bwh.harvard.edu/pph2/>) (Adzhubei et al., 2013), which is tailored to the study of high-throughput Next-Generation Sequencing (NGS) data and features multiple sequence alignments and classifiers based on machine learning; Combined Annotation Dependent Depletion (CADD) (<https://cadd.gs.washington.edu/>) that is designed to estimate the deleterious effect of residue variation on protein sequences (Rentzsch et al., 2019); Rare Exome Variant Ensemble Learner (REVEL) (<https://sites.google.com/site/revelgenomics/>) (Ioannidis et al., 2016); MetaLR (<https://sites.google.com/site/jpopgen/dbNSFP>) which predicts the deleteriousness of missense variants using logistic regression, which incorporates nine independent variant deleteriousness scores and allele frequency information (Liu et al., 2016); Mutation Assessor (<http://mutationassessor.org/r3/>) uses the evolutionary conservation of the impacted residues in protein homologs to speculate on the functional consequences of residue changes in proteins (Reva et al., 2011); Functional Analysis Through Hidden Markov Models (FATHMM) which is a high-throughput web server capable of predicting the functional consequences of both coding variants, that is, non-synonymous single nucleotide variants (nsSNVs) and non-coding variants in the human genome (<http://fathmm.biocompute.org.uk/>); and Predict-SNP (<https://loschmidt.chemi.muni.cz/predictsnp1/>) (Bendl et al., 2014).

## 2.3 Structure-based analyses for point mutation

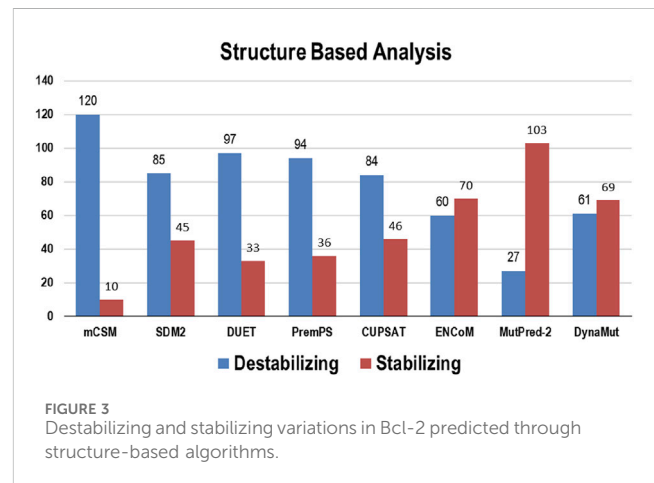
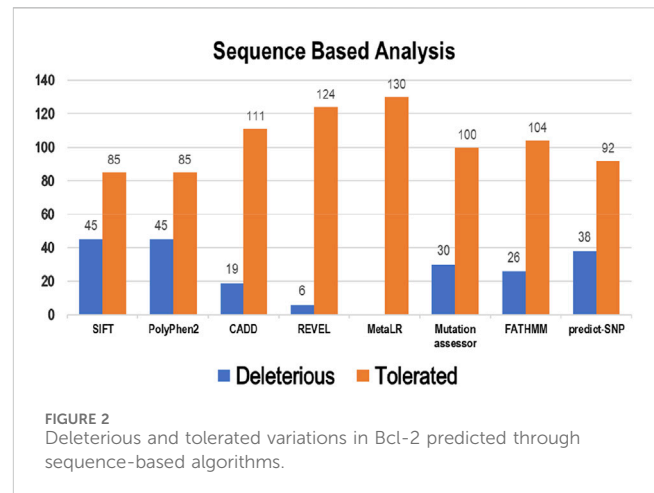
Various algorithms were employed to predict the effect of missense mutations on the protein stability. These include, mCSM (<https://biosig.lab.uq.edu.au/mcsm/>) which uses various residues atomic distance patterns to train the predictive models (Pires et al., 2014a); Site-directed mutator2 (SDM2) (<http://marid.bioc.cam.ac.uk/sdm2>) which can also estimate the relative stability of wild-type and mutated protein structures by comparing them to known homologous 3D structures; DUET (<http://biosig.unimelb.edu.au/duet/>) which uses Support Vector Machines (SVM) to produce a consensual estimate (Pires et al., 2014b); PremPS (<https://lilab.jysw.suda.edu.cn/research/PremPS/>) which estimates changes in the Gibbs free energy of protein unfolding to assess the impact of single mutations on protein stability (Chen et al., 2020); CUPSAT (<http://cupsat.tu-bs.de/>) (Parthiban et al., 2006); ENCoM (<https://labworm.com/tool/encom>) (Frappier et al., 2015); MutPred2 (<http://mutpred.mutdb.org/>) (Pejaver et al., 2020); and DynaMut (<https://biosig.lab.uq.edu.au/dynamut/>) which takes the changes in vibrational entropy into account (Rodrigues et al., 2018).

## 2.4 Disease phenotype prediction analysis

Several machine learning and neural network algorithms were employed for disease phenotype prediction. These include, PhD-SNP (<https://bio.tools/phd-snp>) which uses neural networks that have been trained on a large library of standard and pathogenic mutations (Capriotti and Fariselli, 2017); Protein ANALYSIS THrough Evolutionary Relationships (PANTHER) (<http://www.pantherdb.org/>) which is designed to estimate the likelihood of a particular non-synonymous (residue changing) coding SNP that causes a functional impact on the protein (Thomas et al., 2022); SNPs and GO (<https://snps.biofold.org/snps-and-go/>) is another a precise technique that uses the associated protein functional annotation to determine whether or not a variation is associated with a disease based on a protein sequence (Capriotti et al., 2013); PMut (<http://mmb.irbbarcelona.org/PMut/>) which identifies pathogenic protein variants with up to 80% predictive accuracy in humans (López-Ferrando et al., 2017); and Meta-SNP (<https://snps.biofold.org/meta-snp/>) which is a randomised forest-based classification algorithm that distinguishes between polymorphic non-synonymous SNVs and disease-related one.

## 2.5 Post-transcriptional modification (PTM) sites prediction

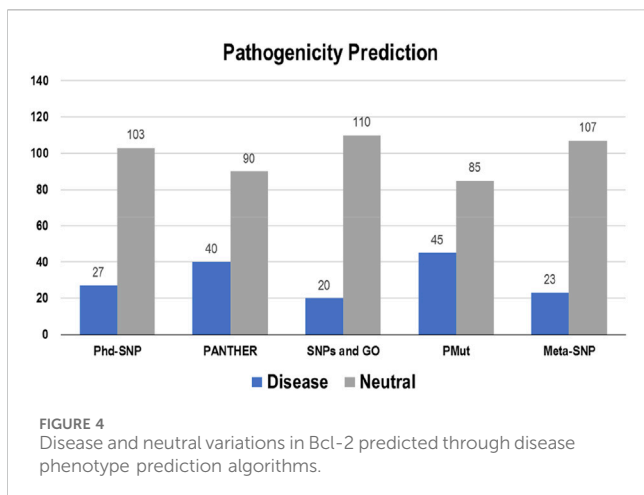
PTM site predictions comprised several rearranged residues that produced many proteins. Ubiquitination, phosphorylation, and methylation are some of the PTM sites that have been characterised. These sites are essential in vital cellular organising processes such as pathological signaling cascades and protein-protein interactions. Thus, PTM prediction assisted in elucidating



whether genetic variants were associated with or contributed to disease pathogenesis. We used four tools for this purpose, namely; NetPhos 3.1 (<https://services.healthtech.dtu.dk/service.php?NetPhos-3.1>); Group-based Prediction System (GPS) 6.0 (<http://gps.biocuckoo.cn/>) (Xue et al., 2005); BDM-PUB (<http://bdmpub.biocuckoo.org/>) which is for protein ubiquitination site prediction using the Bayesian Discriminant Method; and UbPred (<http://www.ubpred.org/>).

## 2.6 Gene-gene interaction network analysis

The gene function can be better understood by studying the genes with which it interacts. The GeneMANIA and STRING databases were used to investigate the relationship between the Bcl-2 gene and other genes and to predict the effect of Bcl-2 nsSNPs on other associated genes. GeneMANIA (<https://genemania.org/>) is a database for identifying genes related to input genes using an extensive set of functional association data (Warde-Farley et al., 2010). These association data included co-expression, colocalisation, pathways, protein domain similarity, and interactions between proteins and genes. GeneMANIA can identify novel pathway members or complex members, genes missed during the screening process, or



genes that perform a specific function, such as protein kinases. STRING (<https://string-db.org/>) is a database of both experimentally verified and theoretically predicted interactions between proteins (Szkarczyk et al., 2021). In STRING, and to ensure high reliability, “physical interactions” and “confidence” was set to 0.99. These interactions occur through computational prediction, inter-organism information transmission, and aggregation of interactions from other (primary) databases, and they can be either direct (physical) or indirect (functional).

### 2.7 Effect of point mutation on the structural and functional integrity of the protein

The formation of a protein complex is critical in controlling many biological activities. Therefore, different algorithms were employed to investigate the effect of Bcl-2<sup>G101V</sup> and Bcl-2<sup>F104L</sup> structural and functional properties. mCSM-PPI2 ([http://biosig.unimelb.edu.au/mcsm\\_ppi2/](http://biosig.unimelb.edu.au/mcsm_ppi2/)) was used to predict the effects of missense mutations on protein-protein affinity (Rodrigues et al., 2019). mCSM-PPI2 uses

graph-based structural signatures to model the effects of variations on the inter-residue interaction network, evolutionary information, complex network metrics, and energy terms to generate an optimised predictor. ConSurf (<https://consurf.tau.ac.il/>) is another tool we employed to estimate the evolutionary conservation of residue positions in a protein molecule based on the phylogenetic relationships between homologous sequences (Ashkenazy et al., 2016). The degree to which the residue position is evolutionarily conserved strongly depends on its structural and functional importance. The ConSurf value varied from 1 to 9, with one denoting residues with the least conservation and nine denoting residues with the most conservation. Other tools such as FTSite (<https://ftsit.bu.edu/>) (Ngan et al., 2012), HOPE (<https://www3.cmbi.umcn.nl/hope/>) and Stride (<http://webclu.bio.wzw.tum.de/stride/>) (Heinig and Frishman, 2004), were also used to provide deeper insight on the structural and functional integrity of the protein upon mutation.

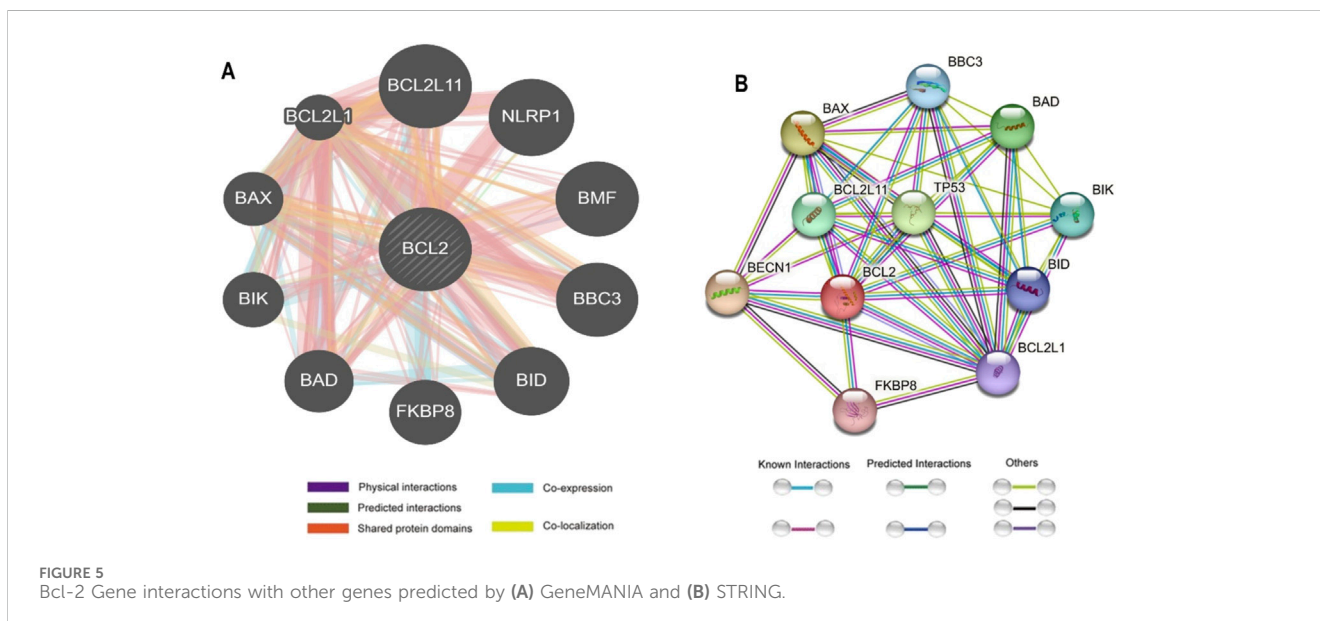
## 2.8 Molecular dynamics (MD) simulations

### 2.8.1 Systems preparation

The Protein Data Bank Repository (RCSB PDB) (<https://www.rcsb.org/>) provided a crystallized X-ray structure of the Bcl-2<sup>WT</sup>, Bcl-2<sup>G101V</sup>, and Bcl-2<sup>F104L</sup> with PDB entries of 6O0K, 6O0L, and 6O0M, respectively. The water molecules in the crystal structure were removed, and the missing hydrogen atoms were substituted for them, with the correct charges assigned at neutral pH. The Schrödinger suite’s Protein Preparation Wizard was employed for initial structure processing and energy minimization. To further reduce steric clashes between residues, we used the OPLS-2005 force field to minimize energy while setting the RMSD threshold to 0.30 for all structures (Shivakumar et al., 2012).

### 2.8.2 Molecular dynamics simulations and post-dynamic analysis

MD simulations were carried out using AMBER18 software and its Particle Mesh Ewald Molecular Dynamics (PMEMD) module



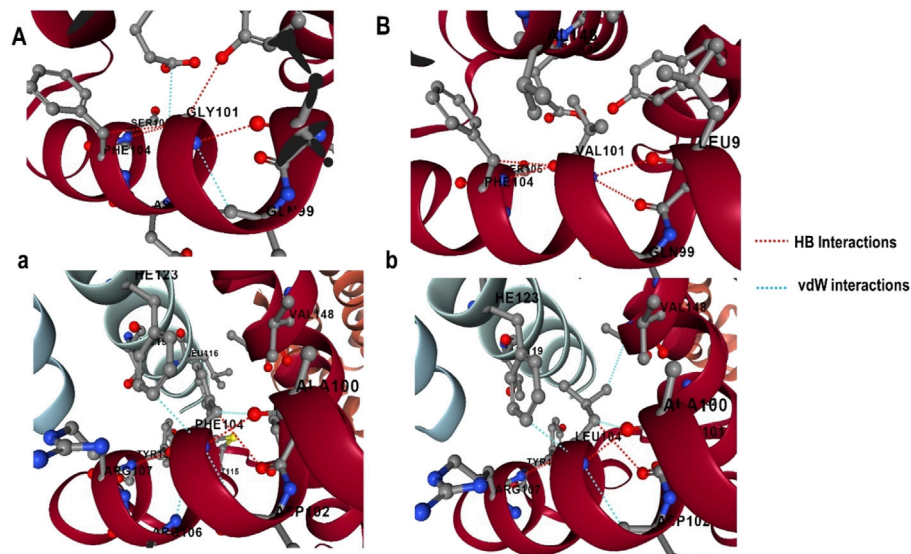


FIGURE 6  
G101 and F104 residue interactions network of Bcl-2; (A) wild G101, (A) G101V variant, (B) wild F104, and (B) F104L variant as predicted by mCSM-PPI2.

(Case et al., 2024; Darden et al., 1993). Protein systems were modelled, and atomic charges were assigned state using the standard Amber (FF14SB) force field within the Amber package. An *in-house* pdb4amber script was used to modify, rename, and protonate (histidine) Bcl-2 (Maier et al., 2015). The LEAP module was employed to generate Bcl-2 parameters and topology files. This was also used for system neutralization. Molecular minimisation was carried out using a constraint potential of 500 kcal/mol, with partial minimisation for 2,500 steps and full minimization taking 5,000 steps. Furthermore, a gradual heating from 0 to 310 K was implemented in the system. The unconstrained equilibration was performed for 5 ns while the atmospheric pressure was maintained at 1 bar with the help of a Berendsen barostat (Berendsen et al., 1984). Subsequently, production stages were conducted over 500 ns to understand the structural consequences of the mutations on Bcl-2.

The enzyme coordinates of Bcl-2<sup>WT</sup>, Bcl-2<sup>G101V</sup>, and Bcl-2<sup>F104L</sup> were saved every 1 ps, and their resultant trajectories were analysed using the AMBER18 integrated CPPTRAJ module (Roe and Cheatham, 2013). Post-MD analyses included root-mean-square deviation (RMSD), root-mean-square fluctuations (RMSF), radius of gyration (Rg), solvent accessible surface area (SASA), intramolecular hydrogen bonding, and dynamic cross-correlation matrix (DCCM). Furthermore, principal component analysis (PCA) was calculated to unravel the protein's atomic displacement extent. The generated data and subsequent complexes were visualized using Microcal Origin analytical software ([www.originlab.com](http://www.originlab.com)), NMWiz implemented in Visual Molecular Dynamics (VMD) (<https://www.ks.uiuc.edu/Research/vmd/>) (Seifert, 2014; Humphrey et al., 1996).

### 3 Results

The Bcl-2 SNP dataset was obtained from the dbSNP and Ensembl databases. Approximately 52,619 variations in Bcl-2 have

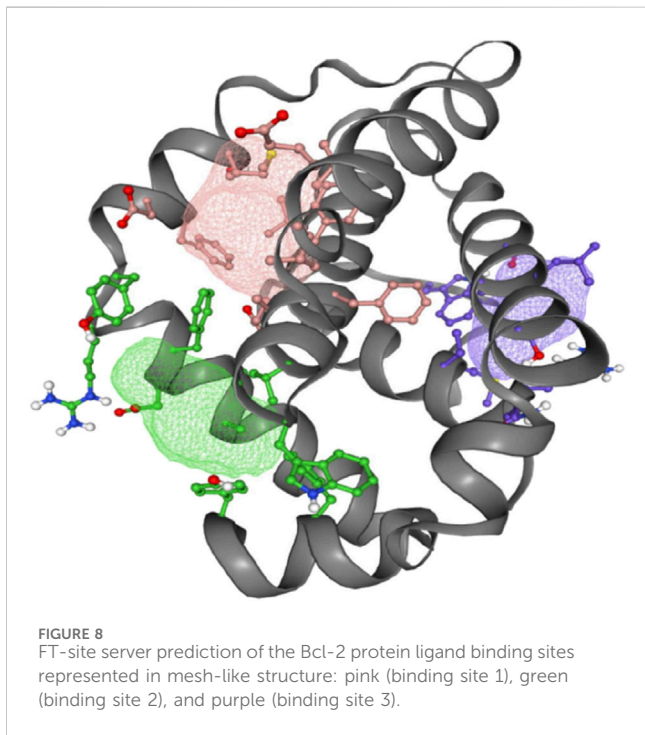
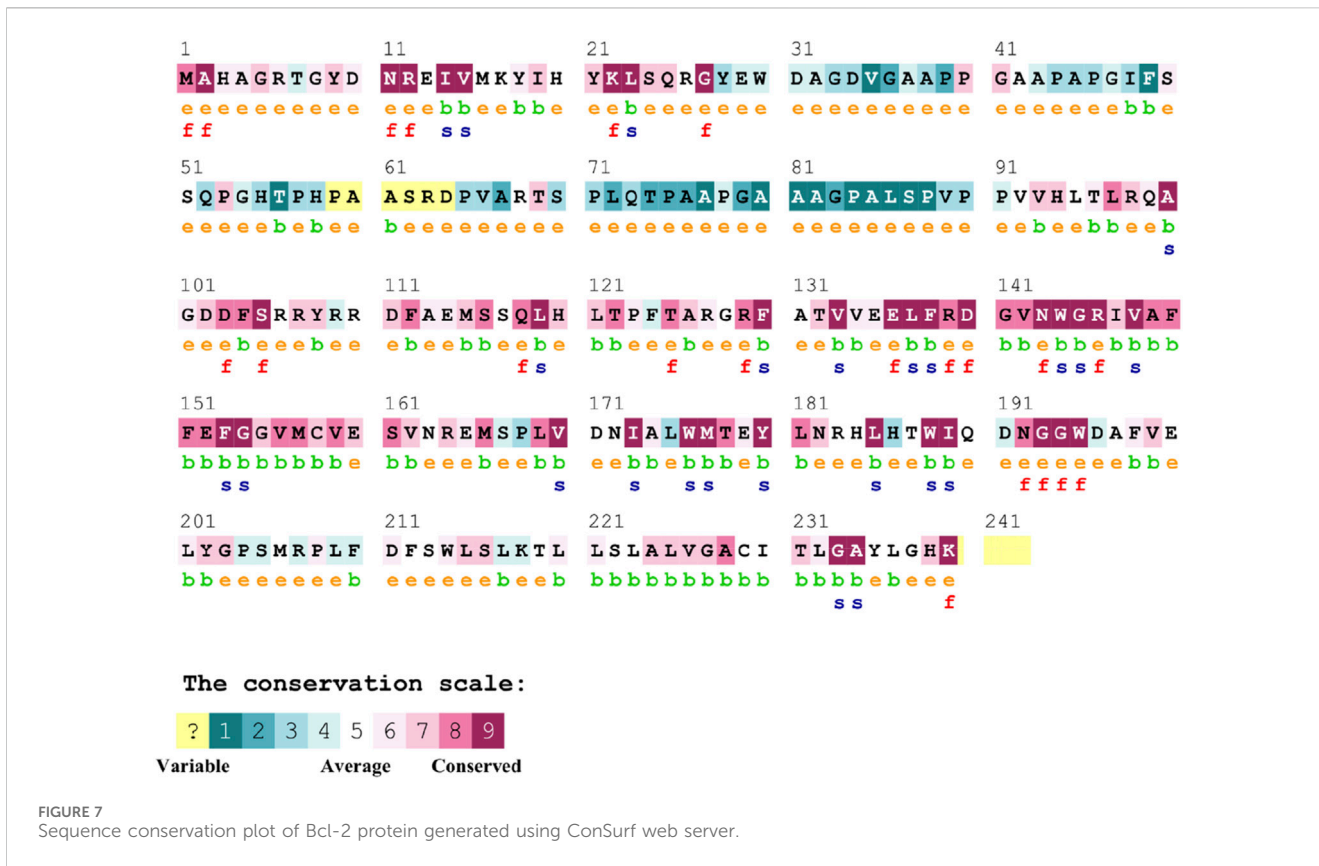
been identified, with 49,593 SNPs located in the intronic region, 163 SNPs classified as missense variants, 1,401 SNPs located in the 3'UTR area, 832 SNPs located in the 5'UTR region, and 115 synonymous variants, as reported by dbSNP and Ensembl. Missense mutations in the coding region were the current target of this study. As a result of further filtering to remove duplicate variations, 130 variants were selected for further investigation.

#### 3.1 Sequence-based analysis of point mutation

Eight tools, namely, SIFT, PolyPhen2, CADD, REVEL, MetaLR, Mutation Assessor, FATHMM, and Predict-SNP were used to conduct sequence-based prediction and analyze the potential effects of Bcl-2 mutations. These eight tools separated deleterious mutations from tolerated ones (Supplementary Table S1). Out of 130 variants, SIFT and PolyPhen2 estimated 45 (~35%) to be deleterious while CADD, REVEL, Mutation Assessor, FATHMM, and Predict-SNP predicted 19 (~15%), 6 (~5%), 30 (~23%), 26 (~20%), and 38 (~29%) mutations as deleterious, respectively. However, the MetaLR algorithm predicted that all 130 (100%) variants were tolerated (Figure 2).

#### 3.2 Structure-based analysis

Multiple computational algorithms, including mCSM, SDM2, DUET, PremPS, CUPSAT, ENCoM, MutPred-2, and DynaMut were used to provide structure-based predictions of the effect of mutations. These tools distinguished between destabilizing and stabilizing mutations (Supplementary Table S2). The analysis concluded that out of 130 mutations, mCSM: 120 (~92%), SDM2: 85 (~65%), DUET: 97 (~75%), PremPS: 94 (~72%),



CUPSAT: 84 (~65%), ENCoM: 60 (~46%), MutPred: 2–27 (~21%), and DynaMut: 61 (~47%) mutations were estimated to be destabilizing the structure of the protein (Figure 3).

### 3.3 Disease phenotype analysis

The pathogenicity of the targeted mutations was assessed utilizing PhD-SNP, PANTHER, SNPs and GO, PMut, and Meta-SNP. These algorithms use their prediction values to determine whether a specific mutation is disease-causing or neutral. From the 130 mutations, PhD-SNP predicted 27 (~21%) mutations to be pathogenic, while PANTHER, SNPs and GO, PMut, and Meta-SNP predicted 40 (~31%), 20 (~15%), 45 (~35%), and 23 (~18%) mutations associated with the disease, respectively (Figure 4). However, only 11 of these mutations were predicted to be disease-causing across all the prediction algorithms (R12G, V15L, H94P, L97P, R98L, R129P, G141E, V142G, N143S, M166T, and G193R) (Supplementary Table S3).

### 3.4 Post-transcriptional modification (PTM) sites prediction

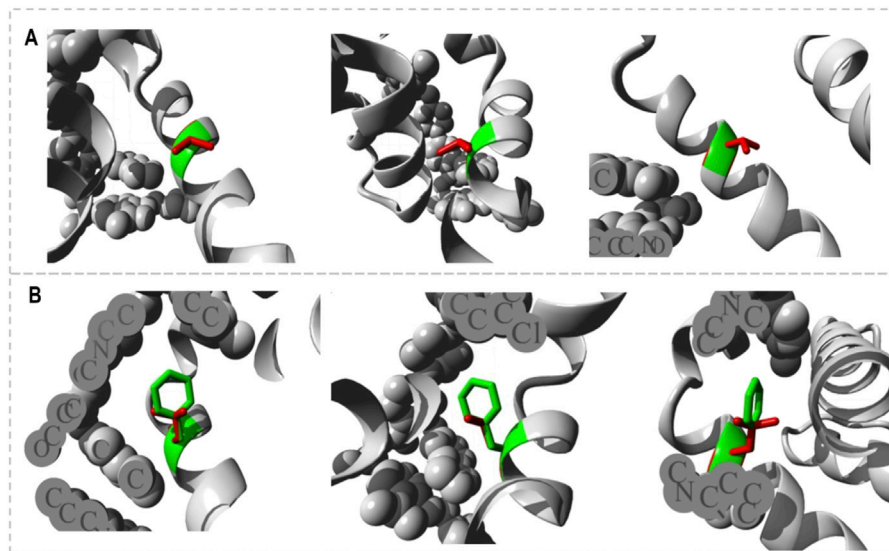
GPS-MSP 6.0 was used for methylation and determined the number of Bcl-2 sites that would be modified. However, GPS-MSP 6.0 predicted that phosphorylation would occur at 35 residues [Ser: 15 (43%), Thr:12 (34%), and Tyr:8 (23%)]. In contrast, it was predicted by Netphos 3.1 those 20 different residues could be phosphorylated [Ser:11 (55%), Thr:7 (35%), and Tyr:2 (10%)].

Ubiquitination was predicted using BDMPUB and UbPred. BDMPUB anticipated that two lysine residues would be ubiquitinated, whereas UbPred projected those four lysine residues would be ubiquitinated.



TABLE 1 Bcl-2 protein ligand-binding sites and their respective residues.

Binding site 1 (pink)	Binding site 2 (green)	Binding site 3 (purple)
Phe104, Asp111, Phe112, Met115, Ser116, Val133, Glu136, Leu137, Ala149, Phe150, Glu152, Phe153, and Val156	Ala100, Gly101, Asp103, Phe104, Arg107, Tyr108, Trp144, Gly145, Val148, Phe198, and Tyr202	Asn11, Arg12, Val15, Met16, Trp30, Asp171, Ala174, Leu175, and Thr178

FIGURE 9 Close-ups (different angles) of the mutant and wild system; (A) Bcl-2<sup>G101V</sup> and (B) Bcl-2<sup>F104L</sup>.

### 3.5 Gene interaction network

The interaction between Bcl-2 and other genes was evaluated using the GeneMANIA and STRING web servers. GeneMANIA analysis showed that Bcl-2 physically interacted with all ten genes and has no co-localization or genetic interaction with any other gene. However, Bcl-2 was co-expressed with BAX, BCL2L1, NLRP1, BBC3, and BID. Moreover, Bcl-2 shared protein domains with BCL2L1, BAX, BIK, and BID (Figure 5A).

The STRING database offers an integrated and comprehensive evaluation of indirect (functional) and direct (physical) protein-protein interactions. The network analysis revealed that Bcl-2 interacted directly 17 genes: BECN1, BAX, TP53, BAD, BCL2L11, BIK, BAK1, BBC3, BID, BCL2L1, HBK, BAG1, MCL1, APAF1, CREB1, NR4A1, and FKBP8 (Figure 5B).

### 3.6 Effect of mutations on the structural and functional integrity of Bcl-2

#### 3.6.1 Estimation of impact of mutation on protein-protein interactions (PPIs)

The effect of mutations on the binding affinity of protein interactions was evaluated using mCSM-PPI2, which evaluates the effect of mutation by simulating the impact of variations on the network of non-covalent interactions between residues utilizing graph kernels, energetic terms, complex network metrics, and

evolutionary data. The decreased binding affinity of protein-protein interaction was observed at the active site residues of the mCSM-PPI2-predicted Bcl-2 interaction, with a change in affinity ( $\Delta\Delta G_{\text{affinity}}$ ) of  $-0.559$  kcal/mol for the G101V variant and  $-1.053$  kcal/mol for the F104L variant. The interaction network revealed that the wild-type protein residue Gly101 established hydrogen bonds with Tyr18, Leu97, Arg98, Phe104, and Ser105, as well as van der Waals interactions with Gln99 and Glu152; however, in the mutant, Val101 established a hydrogen bond with Leu97, Arg98, Phe104, Ser105, and Glu152 (Figure 6). Likewise, the Phe104 in the wild-type generated hydrogen bonds with Ala100, Gly101, and Tyr108, and van der Waals interactions with Ala100, Asp102, Arg106, Tyr108, and Phe123, while in the mutant, leucine formed hydrogen bonds with the same residues in the wild-type (Figure 6).

#### 3.6.2 Conservation analysis of Bcl-2

The conservation of residues is the primary factor that ensures the structural integrity of proteins. The Bcl-2 structure's conservation of residues was investigated using the ConSurf web server to comprehend its significance and localized evolution. The arrangement of residues and their degree of conservation was uncovered utilizing the ConSurf analysis. Several residues in Bcl-2 were shown to be relatively conserved using ConSurf, with particular emphasis on G101 and F104, suggesting that genetic variations at these positions might substantially impact Bcl-2 (Figure 7).



FIGURE 10 The secondary structural analysis of the Bcl-2<sup>WT</sup>, Bcl-2<sup>G101V</sup>, and Bcl-2<sup>F104L</sup> at 10, 100, 200, 300, 400, and 500 ns using the STRIDE web server.

### 3.6.3 Mapping ligand binding sites of Bcl-2

The FT-site web server was used to identify Bcl-2 binding sites based on experimental evidence. The FT-site server depicted three ligand sites in Bcl-2. The ligand sites in Bcl-2 were represented by three different mesh-like structures on the FT-site server (pink, green, and purple), with corresponding residues that are within 5.0 Å of the binding site represented by ball and stick in these sites (Figure 8). The position of the F104 residue is detected in the first and second ligand-binding sites, while G101 is detected in the second ligand-binding site (Table 1). Consequently, mutations G101V and F104L may be more deleterious, as they potentially impact the Bcl-2 ligand-binding affinity.

The HOPE project PDB viewer was used to visualize the structural features of the Bcl-2<sup>WT</sup>, Bcl-2<sup>G101V</sup>, and Bcl-2<sup>F104L</sup> (Figure 9). Each residue demonstrated a unique size, charge, and hydrophobicity. These values frequently varied between the original wild-type and the newly introduced mutant residues. For the Bcl-2<sup>G101V</sup>, the mutant residue was bigger and more hydrophobic than the Bcl-2<sup>WT</sup> residue. Although the mutated residue is not directly involved in ligand binding, it may indirectly affect ligand interactions made by other residues due to changes in local stability. The mutated residue is located within a special BH3 motif. Therefore, the different properties of residues caused the motif to become disrupted and consequently impair its function. Glycine had the highest degree of flexibility compared to other

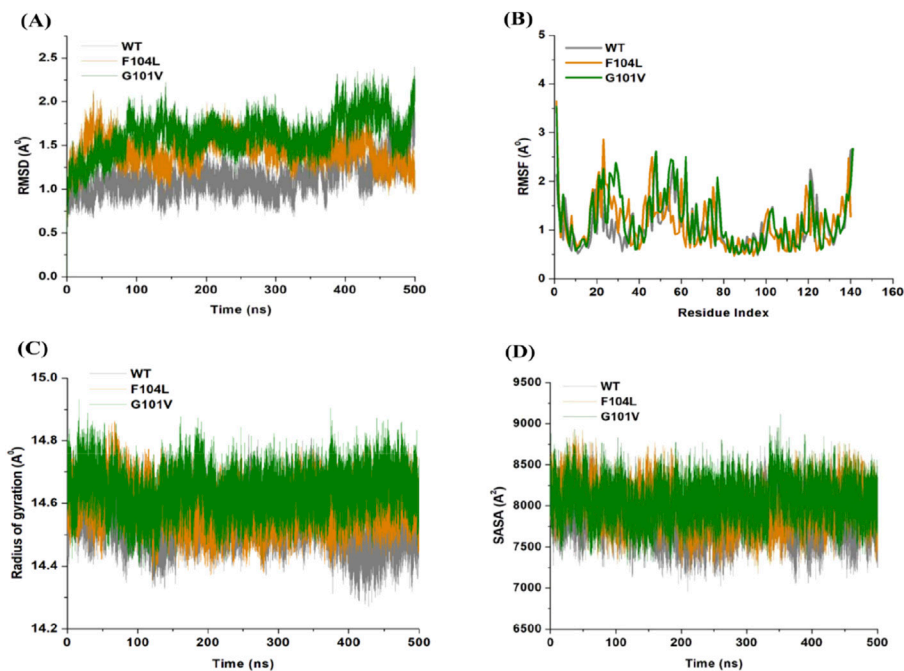


FIGURE 11 (A) RMSD, (B) RMSF, (C) Rg, and (D) SASA values across C $\alpha$  of Bcl-2<sup>WT</sup> (gray), Bcl-2<sup>F104L</sup> (orange), and Bcl-2<sup>G101V</sup> (green) over 500 ns MD simulations.

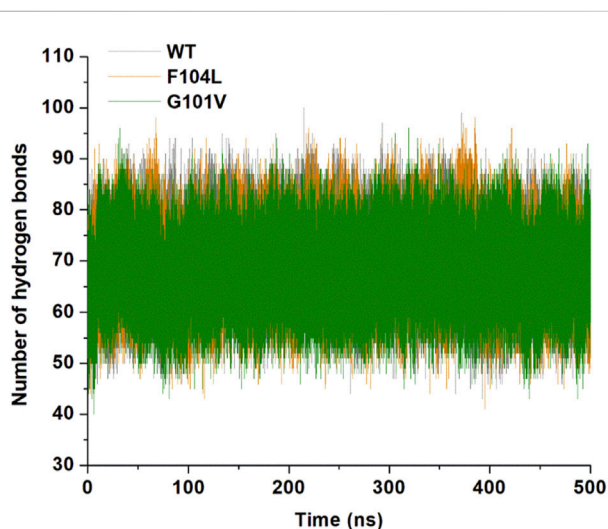


FIGURE 12 Intramolecular hydrogen bonding in Bcl-2<sup>WT</sup> (gray), Bcl-2<sup>F104L</sup> (orange), and Bcl-2<sup>G101V</sup> (green) over 500 ns MD simulations.

residues, which may be necessary for protein function. This function can be abolished by mutating this glycine. For Bcl-2<sup>F104L</sup>, the mutant residue was smaller than the Bcl-2<sup>WT</sup> residue. The Bcl-2<sup>WT</sup> residue interacted with Venetoclax, and the difference in properties between the Bcl-2<sup>WT</sup> and mutant can easily cause a loss of interactions with the ligand. Protein function was frequently dependent on ligand binding, and this mutation may impair this function. The mutated residue was located within a special BH3 motif near a highly

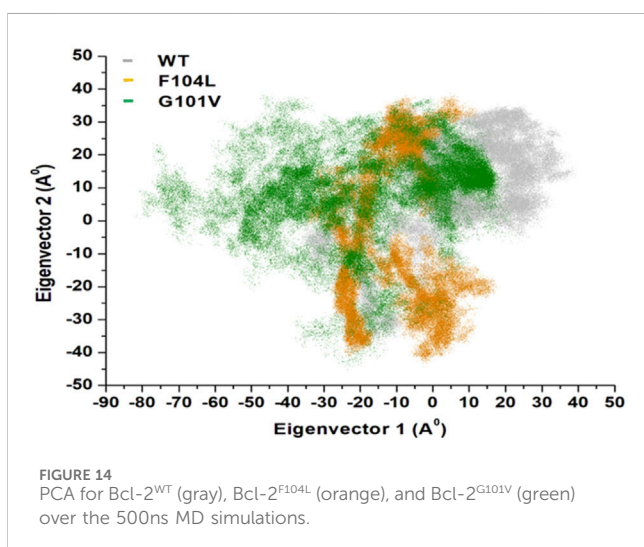
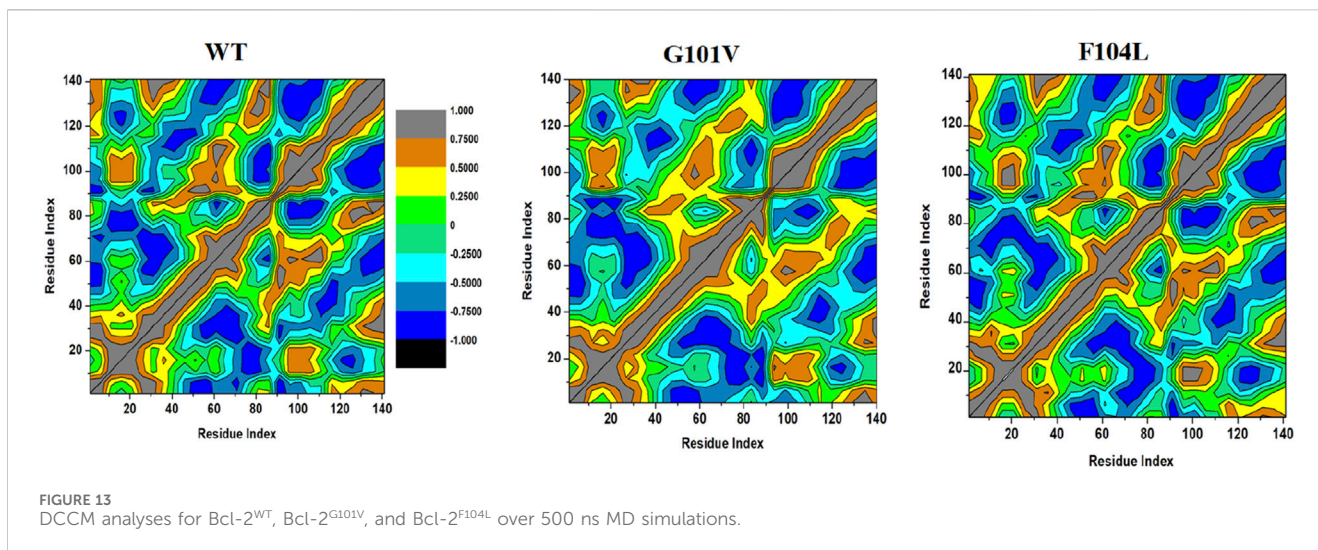
conserved position. Consequently, the motif was disturbed owing to the different properties of the residues, which would impede its function.

### 3.6.4 Investigating the effect of the mutations on the protein secondary structure

MD trajectories of 500 ns were used to investigate the dynamics of secondary structural elements in Bcl-2<sup>WT</sup>, Bcl-2<sup>G101V</sup>, and Bcl-2<sup>F104L</sup>. This study contributed to a better understanding of the effects of genetic variations on the Bcl-2's secondary structure through simulations. The STRIDE web server was used to detect the change in secondary structure at 10, 100, 200, 300, 400, and 500 ns (Figure 10). The secondary structural components in Bcl-2, such as  $\alpha$ -helix, 3–10 helix, and turns, were divided into specific residues at each time interval. The Bcl-2<sup>G101V</sup> and Bcl-2<sup>F104L</sup> were observed to switch from a helix to a turn configuration at these residues.

## 3.7 Dynamic and conformational stability and fluctuations

The inherent behavior of a protein is associated with conformational changes and structural aberrations. Modifying a protein's structure can significantly affect its function]. Therefore, understanding mutation-induced structural changes requires a more in-depth investigation of the conformational dynamics of proteins. For this reason, the effects of Bcl-2 mutations (G101V and F104L) were investigated over 500 ns MD simulations. The dynamics and stability of Bcl-2<sup>WT</sup>, Bcl-2<sup>G101V</sup>, and Bcl-2<sup>F104L</sup> were determined by evaluating the time variable considering the RMSD of



$C_{\alpha}$  atoms from computed trajectories. All systems reached convergence after 100 ns of the simulation period (Figure 11A). The Bcl-2<sup>WT</sup> exhibited the lowest deviated RMSD value, 1.14 Å, while the Bcl-2<sup>G101V</sup> and Bcl-2<sup>F104L</sup> revealed higher RMSD values, 1.43 and 1.62 Å, respectively. The Bcl-2<sup>G101V</sup> disrupted the RMSD pattern of Bcl-2<sup>WT</sup> and caused it to fluctuate more than the Bcl-2<sup>WT</sup> and Bcl-2<sup>F104L</sup> during the simulation. The findings showed that Bcl-2<sup>WT</sup> and Bcl-2<sup>F104L</sup> displayed the least deviation of  $C_{\alpha}$  atoms compared to Bcl-2<sup>G101V</sup>, indicating that the mutation of Gly to Val reduced the structural stability of Bcl-2. Furthermore, no significant variations in structural snaps were noticed, excluding the  $\alpha 3$ - $\alpha 4$  helices (hydrophobic groove) of superimposed Bcl-2<sup>WT</sup>, Bcl-2<sup>G101V</sup>, and Bcl-2<sup>F104L</sup> every 100 ns during the simulation (Supplementary Figure S1). Here,  $\alpha 3$ - $\alpha 4$  helices become more dynamic and flexible as the simulation progresses, thus inducing expansion or shrinking in the hydrophobic groove, which appears most effectively in the Bcl-2<sup>G101V</sup>.

The relative rigidity and flexibility of residues determined protein conformational changes and their associated functions.

Consequently, the RMSF values of Bcl-2<sup>WT</sup>, Bcl-2<sup>G101V</sup>, and Bcl-2<sup>F104L</sup> can be computed and analyzed to see how Bcl-2's residual fluctuations change due to mutations (Figure 11B). Bcl-2<sup>WT</sup> demonstrated the least fluctuations of the residues with an average RMSF value of 1.10 Å when compared to 1.13 and 1.20 Å for the Bcl-2<sup>F104L</sup> and Bcl-2<sup>G101V</sup>, respectively. The calculated trajectory showed a slightly higher pattern of fluctuations, especially for the Bcl-2<sup>G101V</sup> variant. As a result of these mutations, the regions surrounding the various sites become more dynamic and internally disturbed, reflecting higher fluctuations in Bcl-2. The RMSF distribution correlated with the RMSD pattern, with mutated systems exhibiting more significant fluctuations. The substantial variations in the mutants' residual fluctuations could be attributed to Bcl-2 structural inactivation.

Furthermore, the Rg values of all three systems were analyzed to determine the folding behavior and overall conformational changes in the Bcl-2 structure before and after mutation induction. The compactness, stability, and folding of a protein can be determined from the change in Rg values over time. The Rg values of the Bcl-2<sup>WT</sup>, Bcl-2<sup>G101V</sup>, and Bcl-2<sup>F104L</sup> were estimated from the MD trajectories and plotted (Figure 11C). Bcl-2<sup>WT</sup> had the lowest Rg value (14.54 Å, while the Bcl-2<sup>F104L</sup> and Bcl-2<sup>G101V</sup> showed slight increases at 14.59 and 14.63 Å, respectively. Altogether, Rg analysis of Bcl-2 revealed that the mutants were less stable, more flexible, and less compact than the native protein.

Moreover, the Bcl-2 structure's hydrophilic and hydrophobic residues were analyzed using SASA. The SASA values for the Bcl-2<sup>WT</sup>, Bcl-2<sup>G101V</sup>, and Bcl-2<sup>F104L</sup> were obtained and plotted throughout the 500 ns of MD simulation (Figure 11D). Following exposing the system to the solvent, Bcl-2<sup>WT</sup> had a median SASA value of 7,824 Å<sup>2</sup>. The Bcl-2<sup>G101V</sup> exhibited a higher SASA value of 8,049 Å<sup>2</sup> than that of the Bcl-2<sup>F104L</sup>, which displayed a value of 7,985 Å<sup>2</sup>. The SASA values of all three systems agreed with the Rg results. The differences in the SASA values for the three systems throughout the simulation reflect Bcl-2 unfolding and folding. The overall SASA values for Bcl-2<sup>WT</sup> and Bcl-2<sup>F104L</sup> were slightly different, suggesting that the structural mutation from Phenylalanine to Leucine at position 104 in Bcl-2 provides better exposure to solvent compared with

Bcl-2<sup>G101V</sup> and, thus, favors the enhanced activity of the Bcl-2<sup>F104L</sup> over that of the Bcl-2<sup>G101V</sup>.

### 3.7.1 Hydrogen bonding analysis

Analysis of intramolecular hydrogen bonds primarily assists in evaluating the overall conformation and stability of the protein structure through MD simulations. Time-dependent intramolecular hydrogen bond analysis was performed and plotted to evaluate the effect of mutations on the structure of Bcl-2 (Figure 12). The average values of intramolecular hydrogen bonds in Bcl-2<sup>WT</sup>, Bcl-2<sup>G101V</sup>, and Bcl-2<sup>F104L</sup> ranged from about (43–100), (41–98), and (40–96), respectively, indicating a slight change before and after mutation formation. The Bcl-2<sup>F104L</sup> and Bcl-2<sup>WT</sup> models were more compact and stable than the Bcl-2<sup>G101V</sup> model, and the results maintained a roughly similar trajectory pattern.

### 3.7.2 Dynamic cross-correlation matrix (DCCM)

To examine the differences in the dynamics of Bcl-2<sup>WT</sup>, Bcl-2<sup>G101V</sup>, and Bcl-2<sup>F104L</sup>, DCCM plots were generated for anti-correlated and correlated protein structural motions. The residues' motion values range from  $-1$  to  $+1$ . Positive values indicate positively correlated motions (brown colour), whereas negative values indicate anticorrelated motions (black colour) between residues (Figure 13). The scatter plots revealed that motion modes between residues of Bcl-2<sup>F104L</sup> are similar to those of Bcl-2<sup>WT</sup>, whereas the Bcl-2<sup>G101V</sup> showed a slightly different pattern, mutation obviously enhances the positively correlated motions occurring in the Bcl-2.

### 3.7.3 Principal component analysis (PCA)

Intensive movements in Bcl-2<sup>WT</sup>, Bcl-2<sup>G101V</sup>, and Bcl-2<sup>F104L</sup> were evaluated using PC analysis with the first two eigenvectors (EVs) to qualitatively examine the influence of induced mutations on the major conformational movements of each residue (Kumalo et al., 2016). The eigenvectors illustrate the directions of Bcl-2 motion, and the eigenvalues represent the overall motion strength; these are obtained by diagonalizing the covariance matrix (Chen et al., 2021; Chen et al., 2022). The conformational changes of Bcl-2 and its variants were shown in a 2D scatter plot (Figure 14), indicating a significant change in Bcl-2 overall movements after acquiring the mutations, especially Bcl-2<sup>G101V</sup>. Moreover, Figure 14 shows that the Bcl-2<sup>G101V</sup> and Bcl-2<sup>F104L</sup> with the trace covariance matrix of 12.46 and 22.46 Å<sup>2</sup>, respectively, imposed highly fluctuated anti-correlated effects as the negative values of 2D scatter point into the protein. In the case of Bcl-2<sup>WT</sup>, the trace covariance matrices were 24.09 Å<sup>2</sup>, indicating the presence of prominent correlated motions with minimal system fluctuations. Consequently, the findings demonstrated that the Bcl-2<sup>G101V</sup> caused substantial fluctuations in the simulated Bcl-2 dynamics.

## 4 Discussions

### 4.1 Sequence, structure, phenotype-mutational analysis and gene interactions

To ascertain the deleterious effect of residue mutation on the protein, we employed various sequence-based point mutation

algorithms. Out of 130 mutations, SIFT and PolyPhen2 algorithms displayed the highest estimation, deeming 45 mutations (~35%) deleterious. With the exception of the MetaLR algorithm, which predicted that all 130 (100%) variants were tolerated, other algorithms displayed results ranging from around 5 to 23 percent (Figure 2). We hypothesize that the inclusion of machine learning and high-throughput Next-Generation Sequencing (NGS) data in the PolyPhen2 method broadened the search field, contributing to the high prediction rate. Similarly, various algorithms were adopted to predict the effect of missense mutations on the protein stability, and to distinguish between destabilizing and stabilizing mutations. Out of 130 mutations, 3 algorithms (ENCoM, MutPred, and DynaMut) assessed between 21% and 46% of mutations are destabilizing, while 4 predictive tools (mCSM, SDM2, DUET, PremPS, and CUPSAT) estimated between 65% and 92% of mutations are destabilizing (Figure 3). We believe that the analysis adopted here is robust and reliable as we opted to combine various algorithms that take into account critical structural features such as protein folding and Gibbs's free energy (PremPS), site-directed mutations relative to wild type (SDM2), vibrational entropy (DynaMut) and consensual estimation (DUET). A number of machine learning and neural network techniques were used to predict disease phenotypes (Figure 4; Supplementary Table S3), yet only 11 mutations were shown to be disease-causing by all prediction algorithms. These mutations are R12G, V15L, H94P, L97P, R98L, R129P, G141E, V142G, N143S, M166T, and G193R. GeneMANIA and STRING database offer an integrated and comprehensive evaluation of indirect (functional) and direct (physical) protein-protein interactions. The network analysis revealed that Bcl-2, Bcl-2 shared protein domains with BCL2L1, BAX, BIK, and BID (Figure 5A), and interacted directly with BECN1, BAX, TP53, BAD, BCL2L11, BIK, BAK1, BBC3, BID, BCL2L1, HBK, BAG1, MCL1, APAF1, CREB1, NR4A1, and FKBP8 (Figure 5).

### 4.2 Impact of mutations on protein-protein interactions

To explore the impact of Bcl-2<sup>G101V</sup> and Bcl-2<sup>F104L</sup> on their structural and functional characteristics, we utilized various techniques. The mCSM-PPI2 algorithm predicted a reduction in the binding affinity of protein-protein interaction, G101V variant change affinity ( $\Delta\Delta G_{\text{affinity}}$ ) with  $-0.559$  kcal/mol, compared with  $-1.053$  kcal/mol for F104L variant. According to the interaction network, Gly101 in the wild-type protein, generated hydrogen bonds with Tyr18, Leu97, Arg98, Phe104, and Ser105, and exhibited van der Waals interactions with Gln99 and Glu152. However, in the mutant, Val101 established hydrogen bonds with Leu97, Arg98, Phe104, Ser105, and Glu152 (Figure 6). Furthermore, in the wild-type, Phe104 established hydrogen bonds with Ala100, Gly101, and Tyr108 and van der Waals interactions with Ala100, Asp102, Arg106, Tyr108, and Phe123. While in the mutant, leucine established hydrogen bonds with the same residues (Figure 6). The ConSurf web server was utilized to confirm

the structural integrity of the Bcl-2 protein. Several residues in the Bcl-2 protein were shown to be relatively conserved, with a specific focus on G101 and F104., suggesting that genetic variations at these positions might substantially impact Bcl-2 (Figure 7). Additionally, FTSite, HOPE, and Stride were employed to gain further understanding of the structural and functional integrity of the Bcl-2 protein following mutation. The FT-site server depicted three ligand sites in Bcl-2 (Figure 8). According to Table 1, the first and second ligand-binding sites detect the position of the F104 residue, while the second ligand-binding site detects the G101 residue. Considering they may affect the Bcl-2 ligand-binding affinity, mutations G101V and F104L may thus be more deleterious. The Bcl-2<sup>WT</sup>, Bcl-2<sup>G101V</sup>, and Bcl-2<sup>F104L</sup> structural characteristics were visualized using the HOPE project PDB viewer (Figure 9). The Bcl-2<sup>G101V</sup> mutant residue exhibited a bigger size and greater hydrophobicity compared to the Bcl-2<sup>WT</sup> residue. The mutant residue of Bcl-2<sup>F104L</sup> was smaller than the residue of Bcl-2<sup>WT</sup>. Venetoclax was bound to the Bcl-2<sup>WT</sup> residue, and because the two amino acids had different characteristics, the mutant form of Bcl-2<sup>WT</sup> can readily lose its binding affinity for the ligand. Finally, the STRIDE web server was utilized to identify alterations in the secondary structure at specific time points: 10, 100, 200, 300, 400, and 500 ns (Figure 10). The conformational switch from a helix to a turn was seen in Bcl-2<sup>G101V</sup> and Bcl-2<sup>F104L</sup> at these residues.

### 4.3 Effect of mutations on the structural and dynamic landscape of the protein

We employed the MD simulations to conduct a comprehensive analysis of the conformational dynamics of proteins to understand the structural alterations caused by mutations. These mutations affected Bcl-2's stability, flexibility, solvent-accessible surface area, and rigidity, as demonstrated by 500 ns MD simulations (Figure 11). Moreover, mutations impacted Bcl-2's hydrogen bond formation, and the Bcl-2<sup>F104L</sup> and Bcl-2<sup>WT</sup> models exhibited greater compactness and stability compared to the Bcl-2<sup>G101V</sup> model (Figure 12). To explore mutation-induced effect on conformational alterations of Bcl-2, DCCMs and PCA are estimated. The results showed that the Bcl-2<sup>G101V</sup> mutation clearly affects the positively correlated motions occurring in the Bcl-2 and causes substantial fluctuations in the simulated Bcl-2 dynamics (Figures 13, 14).

Overall, the findings of this study hold several biological significances, for instance having information on SNPs in the Bcl-2 gene would help identify potential biomarkers for cancer diagnosis and treatment. Furthermore, by examining the structural and functional effects of SNPs in Bcl-2, our finding may pinpoint novel targets for cancer therapy. Treatments that specifically target genetic variants or protein interactions linked to Bcl-2 SNPs may be able to return cancer cells to normal apoptotic pathways, which would ultimately result in their elimination. Information presented here on how SNPs in Bcl-2 influence protein-protein interactions can provide insights into the molecular mechanisms underlying cancer development and progression.

## 5 Limitation of the study and future perspective

The current study has focused exclusively on the association between single nucleotide polymorphisms (SNPs) in the Bcl-2 gene and various aspects of its function and interactions in human cells. One limitation of this approach is the exclusion of comparative genomic analyses, which could provide additional insights into the evolutionary history and functional differences between Bcl-2 in cancerous versus non-cancerous cells, as well as comparisons with unicellular organisms such as yeasts. Such comparisons might reveal conserved or divergent evolutionary traits that contribute to our understanding of Bcl-2 role in apoptosis and oncogenesis across different species and cell types. Moreover, the study does not address the broader genomic context that may influence these variations, such as regulatory elements or interactions with other genomic regions. The potential impact of epigenetic factors on Bcl-2 expression and function is also not explored, which could be significant given the gene's role in critical cellular processes.

Future studies could expand on the current work by incorporating comparative genomics to analyze Bcl-2 across different species, including model organisms like yeasts, which can offer valuable insights due to their simpler genetic backgrounds and ease of genetic manipulation. Such studies would enhance our understanding of the evolutionary pressures that have shaped the Bcl-2 gene and could identify conserved elements critical for its function. Additionally, examining the interplay between Bcl-2 SNPs and other genomic or epigenetic factors could provide a more comprehensive picture of how Bcl-2 variants contribute to disease phenotypes. This could involve integrating broader genomic data sets, including whole-genome sequencing and epigenetic profiling, to discern the complex regulatory networks that impact BCL-2 expression and activity. In light of these limitations, further research could also focus on the translational application of our findings, exploring how the SNPs identified could influence the efficacy of BCL-2-targeted therapies in clinical settings.

By addressing these areas, future research could provide a deeper understanding of BCL-2's role in disease and offer new avenues for therapeutic intervention, ultimately leading to improved treatment strategies for diseases mediated by this critical gene.

## 6 Conclusion

This study explored the impact of single nucleotide polymorphisms (SNPs) in the Bcl-2 gene on the protein structural and functional dynamics, with implications for carcinogenesis. Comprehensive bioinformatics tools and molecular dynamics simulations revealed that 8.5% of identified mutations in Bcl-2 were pathogenic, with Bcl-2<sup>G101V</sup> and Bcl-2<sup>F104L</sup> emerging as the most deleterious variants. These mutations significantly disrupted protein stability, binding affinities in protein-protein interactions, and ligand-binding capabilities. Structural and dynamic analyses indicated that these mutations led to conformational deviations, altered secondary structure, and compromised the integrity of critical functional motifs such as the BH3 domain.

The findings underscore the pivotal role of Bcl-2 mutations in disrupting apoptotic regulation, a hallmark of cancer, and highlight

their potential as diagnostic biomarkers and therapeutic targets. By providing a detailed characterization of mutation-induced effects on Bcl-2, this study lays a foundation for future experimental validation and the development of targeted anti-cancer strategies, including rational drug design.

While the current work focuses on the molecular implications of Bcl-2 SNPs, future research integrating broader genomic and epigenetic datasets, as well as comparative analyses across species, will provide a more holistic understanding the role of Bcl-2 in apoptosis and oncogenesis. These efforts could contribute to innovative therapeutic interventions targeting Bcl-2-associated pathways in cancer.

## Data availability statement

The original contributions presented in the study are included in the article/[Supplementary Material](#), further inquiries can be directed to the corresponding author.

## Ethics statement

Ethical approval was not required for the study involving humans in accordance with the local legislation and institutional requirements. Written informed consent to participate in this study was not required from the participants or the participants' legal guardians/next of kin in accordance with the national legislation and the institutional requirements.

## Author contributions

GE: Formal Analysis, Investigation, Methodology, Writing—original draft. ZZ: Writing—review and editing. DD: Writing—review and editing. KK: Writing—review and editing, Software. JM: Writing—review and editing, Investigation, Resources. PM: Writing—review and editing. NM: Writing—review and editing, Supervision. MS: Conceptualization, Funding acquisition, Investigation, Methodology, Project administration, Supervision, Writing—review and editing.

## References

- Adams, J. M., and Cory, S. (2017). The BCL-2 arbiters of apoptosis and their growing role as cancer targets. *Cell Death Differ.* 25 (1), 27–36. doi:10.1038/cdd.2017.161
- Adzhubei, I., Jordan, D. M., and Sunyaev, S. R. (2013). Predicting functional effect of human missense mutations using PolyPhen-2. *Curr. Protoc. Hum. Genet.* 76 (1), 20. doi:10.1002/0471142905.hg0720s76
- Ashkenazy, H., Abadi, S., Martz, E., Chay, O., Mayrose, I., Pupko, T., et al. (2016). ConSurf 2016: an improved methodology to estimate and visualize evolutionary conservation in macromolecules. *Nucleic Acids Res.* 44 (W1), W344–W350. doi:10.1093/nar/gkw408
- Barriuso, D., Alvarez-Frutos, L., Gonzalez-Gutierrez, L., Motiño, O., Kroemer, G., Palacios-Ramirez, R., et al. (2023). Involvement of bcl-2 family proteins in tetraploidization-related senescence. *Int. J. Mol. Sci.* 24 (7), 6374. doi:10.3390/IJMS24076374
- Bateman, A., Martin, M. J., O'Donovan, C., et al. (2017). UniProt: the universal protein knowledgebase. *Nucleic Acids Res.* 45 (D1), D158–D169. doi:10.1093/NAR/GKW1099
- Bendl, J., Stourac, J., Salanda, O., Pavelka, A., Wieben, E. D., Zendulka, J., et al. (2014). PredictSNP: robust and accurate consensus classifier for prediction of disease-related mutations. *PLoS Comput. Biol.* 10 (1), e1003440. doi:10.1371/journal.pcbi.1003440
- Berendsen, H. J. C., Postma, J. P. M., van Gunsteren, W. F., DiNola, A., and Haak, J. R. (1984). Molecular dynamics with coupling to an external bath. *J. Chem. Phys.* 81 (8), 3684–3690. doi:10.1063/1.448118
- Birkinshaw, R. W., Gong, J. nan, Luo, C. S., Lio, D., White, C. A., Anderson, M. A., et al. (2019). Structures of BCL-2 in complex with venetoclax reveal the molecular basis of resistance mutations. *Nat. Commun.* 10 (1), 2385. doi:10.1038/s41467-019-10363-1
- Blomberg, P., Anderson, M. A., Gong, J. N., Thijssen, R., Birkinshaw, R. W., Thompson, E. R., et al. (2019). Acquisition of the recurrent Gly101Val mutation in BCL2 confers resistance to venetoclax in patients with progressive chronic lymphocytic leukemia. *Cancer Discov.* 9 (3), 342–353. doi:10.1158/2159-8290.CD-18-1119
- Blomberg, P., Thompson, E. R., Nguyen, T., Birkinshaw, R. W., Gong, J. N., Chen, X., et al. (2020). Multiple BCL2 mutations cooccurring with Gly101Val emerge in chronic

## Funding

The author(s) declare that financial support was received for the research, authorship, and/or publication of this article. This research was funded by the University of KwaZulu-Natal Research Office.

## Acknowledgments

The authors thank the Centre for High-Performance Computing ([www.chpc.ac.za](http://www.chpc.ac.za)), Cape Town, South Africa, for the computational resources.

## Conflict of interest

The authors declare that the research was conducted in the absence of any commercial or financial relationships that could be construed as a potential conflict of interest.

## Generative AI statement

The author(s) declare that no Generative AI was used in the creation of this manuscript.

## Publisher's note

All claims expressed in this article are solely those of the authors and do not necessarily represent those of their affiliated organizations, or those of the publisher, the editors and the reviewers. Any product that may be evaluated in this article, or claim that may be made by its manufacturer, is not guaranteed or endorsed by the publisher.

## Supplementary material

The Supplementary Material for this article can be found online at: <https://www.frontiersin.org/articles/10.3389/fgene.2024.1502152/full#supplementary-material>

- lymphocytic leukemia progression on venetoclax. *Blood* 135 (10), 773–777. doi:10.1182/BLOOD.2019004205
- Capriotti, E., Calabrese, R., Fariselli, P., Martelli, P., Altman, R. B., and Casadio, R. (2013). WS-SNPs&GO: a web server for predicting the deleterious effect of human protein variants using functional annotation. *BMC Genomics* 14 (Suppl. 3), S6. doi:10.1186/1471-2164-14-S3-S6
- Capriotti, E., and Fariselli, P. (2017). PhD-SNPg: a webserver and lightweight tool for scoring single nucleotide variants. *Nucleic Acids Res.* 45 (W1), W247–W252. doi:10.1093/NAR/GKX369
- Case, D. A., Walker, R. C., Cheatham, T. E., Case, D. A., Walker, R. C., et al. (2024). Amber 2018. *Univ. Calif. San. Fr.* 2018.
- Chatterjee, N., and Walker, G. C. (2017). Mechanisms of DNA damage, repair, and mutagenesis. *Environ. Mol. Mutagen.* 58 (5), 235–263. doi:10.1002/EM.22087
- Chen, J., Zeng, Q., Wang, W., Sun, H., and Hu, G. (2022). Decoding the identification mechanism of an SAM-III riboswitch on ligands through multiple independent Gaussian-accelerated molecular dynamics simulations. *J. Chem. Inf. Model.* 62 (23), 6118–6132. doi:10.1021/acs.jcim.2c00961
- Chen, J., Zhang, S., Wang, W., Pang, L., Zhang, Q., and Liu, X. (2021). Mutation-induced impacts on the switch transformations of the GDP- and GTP-bound K-ras: insights from multiple replica Gaussian accelerated molecular dynamics and free energy analysis. *J. Chem. Inf. Model.* 61 (4), 1954–1969. doi:10.1021/acs.jcim.0c01470
- Chen, Y., Lu, H., Zhang, N., Zhu, Z., Wang, S., and Li, M. (2020). PremPS: predicting the impact of missense mutations on protein stability. *PLoS Comput. Biol.* 16 (12), e1008543. doi:10.1371/journal.pcbi.1008543
- Conway, P. J., Dao, J., Kovalsky, D., Mahadevan, D., and Dray, E. (2024). Polyploidy in cancer: causal mechanisms, cancer-specific consequences, and emerging treatments. *Mol. Cancer Ther.* 23 (5), 638–647. doi:10.1158/1535-7163
- Cory, S., and Adams, J. M. (2002). The Bcl2 family: regulators of the cellular life-or-death switch. *Nat. Rev. Cancer* 2 (9), 647–656. doi:10.1038/nrc883
- Czabotar, P. E., Lessene, G., Strasser, A., and Adams, J. M. (2014). Control of apoptosis by the BCL-2 protein family: implications for physiology and therapy. *Nat. Rev. Mol. Cell Biol.* 15 (1), 49–63. doi:10.1038/NRM3722
- Dakal, T. C., Kala, D., Dhiman, G., Yadav, V., Krokhotin, A., and Dokholyan, N. V. (2017). Predicting the functional consequences of non-synonymous single nucleotide polymorphisms in IL8 gene. *Sci. Rep.* 7 (1), 6525–6618. doi:10.1038/s41598-017-06575-4
- Darden, T., York, D., and Pedersen, L. (1993). Particle mesh Ewald: an N log(N) method for Ewald sums in large systems. *J. Chem. Phys.* 98 (12), 10089–10092. doi:10.1063/1.464397
- Delbridge, A. R. D., and Strasser, A. (2015). The BCL-2 protein family, BH3-mimetics and cancer therapy. *Cell. Death Differ.* 22 (7), 1071–1080. doi:10.1038/cdd.2015.50
- Delbridge, ARDD, Grabow, S., Strasser, A., and Vaux, D. L. (2016). Thirty years of BCL-2: translating cell death discoveries into novel cancer therapies. *Nat. Rev. Cancer* 16 (2), 99–109. doi:10.1038/nrc.2015.17
- Edelman, L. B., Eddy, J. A., and Price, N. D. (2010). *In silico* models of cancer. *WIREs Syst. Biol. Med.* 2 (4), 438–459. doi:10.1002/wsbm.75
- Elamin, G., Aljoundi, A. E. S., and Soliman, M. (2024). From biological activity to stereoselectivity: a portrait of molecular and mechanistic profiles of the therapeutic potential of G-1 and LNS8801 as GPER-1 activator in the treatment of waldenström's macroglobulinemia. *Innov. Discov.* 1, 7. doi:10.53964/id.2024007
- Frappier, V., Chartier, M., and Najmanovich, R. J. (2015). ENCoM server: exploring protein conformational space and the effect of mutations on protein function and stability. *Nucleic Acids Res.* 43 (W1), W395–W400. doi:10.1093/nar/gkv343
- Goff, D. J., Recart, A. C., Sadarangani, A., Chun, H. J., Barrett, C. L., Krajewska, M., et al. (2013). A pan-BCL2 inhibitor renders bone-marrow-resident human leukemia stem cells sensitive to tyrosine kinase inhibition. *Cell. Stem Cell.* 12 (3), 316–328. doi:10.1016/j.stem.2012.12.011
- Heinig, M., and Frishman, D. (2004). STRIDE: a web server for secondary structure assignment from known atomic coordinates of proteins. *Nucleic Acids Res.* 32 (Web Server), W500–W502. doi:10.1093/nar/gkh429
- Hubbard, T., Barker, D., Birney, E., Cameron, G., Chen, Y., Clark, L., et al. (2002). The Ensembl genome database project. *Nucleic Acids Res.* 30 (1), 38–41. doi:10.1093/NAR/30.1.38
- Humphrey, W., Dalke, A., and Schulten, K. (1996). VMD: Visual molecular dynamics. *J. Mol. Graph.* 14 (1), 33–38. doi:10.1016/0263-7855(96)00018-5
- Ichim, G., and Tait, S. W. G. (2016). A fate worse than death: apoptosis as an oncogenic process. *Nat. Rev. Cancer.* 16 (8), 539–548. doi:10.1038/nrc.2016.58
- Ioannidis, N. M., Rothstein, J. H., Pejaver, V., Middha, S., McDonnell, S. K., Baheti, S., et al. (2016). REVEL: an Ensemble method for predicting the pathogenicity of Rare missense variants. *Am. J. Hum. Genet.* 99 (4), 877–885. doi:10.1016/j.ajhg.2016.08.016
- Jiménez-Santos, M. J., García-Martín, S., Fustero-Torre, C., Di Domenico, T., Gómez-López, G., and Al-Shahrouf, F. (2022). Bioinformatics roadmap for therapy selection in cancer genomics. *Mol. Oncol.* 16 (21), 3881–3908. doi:10.1002/1878-0261.13286
- Jin, J., Wu, X., Yin, J., Li, M., Shen, J., Li, J., et al. (2019). Identification of genetic mutations in cancer: challenge and opportunity in the new era of targeted therapy. *Front. Oncol.* 9, 263. doi:10.3389/fgene.2019.00263
- Kalkavan, H., Rühl, S., Shaw, J. J. P., and Green, D. R. (2023). Non-lethal outcomes of engaging regulated cell death pathways in cancer. *Nat. Cancer.* 4 (6), 795–806. doi:10.1038/s43018-023-00571-6
- Karimi, M. R., Karimi, A. H., Abolmaali, S., Sadeghi, M., and Schmitz, U. (2022). Prospects and challenges of cancer systems medicine: from genes to disease networks. *Brief. Bioinform.* 23 (1), bbab343. doi:10.1093/bib/bbab343
- Kitada, S., Pedersen, I. M., Schimmer, A. D., and Reed, J. C. (2002). Dysregulation of apoptosis genes in hematopoietic malignancies. *Oncogene* 21 (21), 3459–3474. doi:10.1038/sj.onc.1205327
- Kucukkal, T. G., Petukh, M., Li, L., and Alexov, E. (2015). Structural and physico-chemical effects of disease and non-disease nsSNPs on proteins. *Curr. Opin. Struct. Biol.* 32, 18–24. doi:10.1016/j.sbi.2015.01.003
- Kumalo, H. M., Bhakat, S., and Soliman, M. E. (2016). Investigation of flap flexibility of  $\beta$ -secretase using molecular dynamic simulations. *J. Biomol. Struct. Dyn.* 34 (5), 1008–1019. doi:10.1080/07391102.2015.1064831
- Kumar, P., Henikoff, S., and Ng, P. C. (2009). Predicting the effects of coding non-synonymous variants on protein function using the SIFT algorithm. *Nat. Protoc.* 4 (7), 1073–1081. doi:10.1038/NPROT.2009.86
- Lavrik, I., Golks, A., and Kramer, P. H. (2005). Death receptor signaling. *J. Cell Sci.* 118 (2), 265–267. doi:10.1242/JCS.01610
- Liu, X., Wu, C., Li, C., and Boerwinkle, E. (2016). dbNSFP v3.0: a one-stop database of functional predictions and annotations for human nonsynonymous and splice-site SNVs. *Hum. Mutat.* 37 (3), 235–241. doi:10.1002/humu.22932
- López-Ferrando, V., Gazzo, A., de la Cruz, X., Orozco, M., and Gelpí, J. L. (2017). PMut: a web-based tool for the annotation of pathologic variants on proteins, 2017 update. *Nucleic Acids Res.* 45 (W1), W222–W228. doi:10.1093/nar/gkx313
- Maier, J. A., Martinez, C., Kasavajhala, K., Wickstrom, L., Hauser, K. E., and Simmerling, C. (2015). ff14SB: improving the accuracy of protein side chain and backbone parameters from ff99SB. *J. Chem. Theory Comput.* 11 (8), 3696–3713. doi:10.1021/acs.jctc.5b00255
- McDonald, P. C., Nagel, J. M., and Dedhar, S. (2021). Anastasis, recovery from the brink of death as a mechanism of drug resistance. *Biological Mechanisms and the Advancing Approaches to Overcoming Cancer Drug Resistance.* 251–260. doi:10.1016/B978-0-12-821310-0.00004-8
- Nano, M., and Montell, D. J. (2024). Apoptotic signaling: beyond cell death. *Semin. Cell Dev. Biol.* 156, 22–34. doi:10.1016/j.semcdb.2023.11.002
- Ngan, C. H., Hall, D. R., Zerbe, B., Grove, L. E., Kozakov, D., and Vajda, S. (2012). FTSite: high accuracy detection of ligand binding sites on unbound protein structures. *Bioinformatics* 28 (2), 286–287. doi:10.1093/bioinformatics/btr651
- Niculescu, V. (2024). Re-Evaluating cancer stem cells (CSCs) and polyploid giant cancer cells (PGCCs) in the light of evolutionary cancer cell biology ECCB. *[Epub ahead of print]*. doi:10.20944/PREPRINTS202409.0026.V1
- Niculescu, V. F. (2024). Understanding cancer from an evolutionary perspective: high-risk reprogramming of genome-damaged stem cells. *Acad. Med. [Epub ahead of print]*. doi:10.20935/ACADMED6168
- Niculescu, V. F., and Niculescu, E. R. (2024). The enigma of cancer polyploidy as deciphered by evolutionary cancer stem cell biology (ECCB). *Acad. Med. [Epub ahead of print]*. doi:10.20935/ACADMED6233
- Parthiban, V., Gromiha, M. M., and Schomburg, D. (2006). CUPSAT: prediction of protein stability upon point mutations. *Nucleic Acids Res.* 34 (Web Server), W239–W242. doi:10.1093/nar/gkl190
- Pejaver, V., Urresti, J., Lugo-Martinez, J., Pagel, K. A., Lin, G. N., Nam, H. J., et al. (2020). Inferring the molecular and phenotypic impact of amino acid variants with MutPred2. *Nat. Commun.* 11 (1), 5918–6013. doi:10.1038/s41467-020-19669-x
- Perini, G. F., Ribeiro, G. N., Pinto Neto, J. V., Campos, L. T., and Hamerschlag, N. (2018). BCL-2 as therapeutic target for hematological malignancies. *J. Hematol. Oncol.* 11 (1), 65. doi:10.1186/s13045-018-0608-2
- Pires, D. E. V., Ascher, D. B., and Blundell, T. L. (2014a). mCSM: predicting the effects of mutations in proteins using graph-based signatures. *Bioinformatics* 30 (3), 335–342. doi:10.1093/bioinformatics/btt691
- Pires, D. E. V., Ascher, D. B., and Blundell, T. L. (2014b). DUET: a server for predicting effects of mutations on protein stability using an integrated computational approach. *Nucleic Acids Res.* 42 (W1), W314–W319. doi:10.1093/nar/gku411
- Qian, S., Wei, Z., Yang, W., Huang, J., Yang, Y., and Wang, J. (2022). The role of BCL-2 family proteins in regulating apoptosis and cancer therapy. *Front. Oncol.* 12, 985363. doi:10.3389/fgene.2022.985363
- Rentsch, P., Witten, D., Cooper, G. M., Shendure, J., and Kircher, M. (2019). CADD: predicting the deleteriousness of variants throughout the human genome. *Nucleic Acids Res.* 47 (D1), D886–D894. doi:10.1093/nar/gky1016
- Reva, B., Antipin, Y., and Sander, C. (2011). Predicting the functional impact of protein mutations: application to cancer genomics. *Nucleic Acids Res.* 39 (17), e118. doi:10.1093/nar/gkr407



- Roberts, A. W., Davids, M. S., Pagel, J. M., Kahl, B. S., Puvvada, S. D., Gerecitano, J. F., et al. (2016). Targeting BCL2 with venetoclax in relapsed chronic lymphocytic leukemia. *N. Engl. J. Med.* 374 (4), 311–322. doi:10.1056/NEJMoa1513257
- Rodrigues, C. H., Pires, D. E., and Ascher, D. B. (2018). DynaMut: predicting the impact of mutations on protein conformation, flexibility and stability. *Nucleic Acids Res.* 46 (W1), W350–W355. doi:10.1093/nar/gky300
- Rodrigues, C. H. M., Myung, Y., Pires, D. E. V., and Ascher, D. B. (2019). mCSM-PPI2: predicting the effects of mutations on protein–protein interactions. *Nucleic Acids Res.* 47 (W1), W338–W344. doi:10.1093/nar/gkz383
- Roe, D. R., and Cheatham, T. E. (2013). PTRAJ and CPPTRAJ: software for processing and analysis of molecular dynamics trajectory data. *J. Chem. Theory Comput.* 9 (7), 3084–3095. doi:10.1021/ct400341p
- Rosser, C. J., Reyes, A. O., Vakar-Lopez, F., Levy, L. B., Kuban, D. A., Hoover, D. C., et al. (2003). Bcl-2 is significantly overexpressed in localized radio-recurrent prostate carcinoma, compared with localized radio-naïve prostate carcinoma. *Int. J. Radiat. Oncology\*Biolog\*Physic* 56 (1), 1–6. doi:10.1016/S0360-3016(02)04468-1
- Seifert, E. (2014). OriginPro 9.1: scientific data analysis and graphing software-software review. *J. Chem. Inf. Model.* 54 (5), 1552. doi:10.1021/ci500161d
- Sherry, S. T., Ward, M. H., Kholodov, M., Baker, J., Phan, L., Smigielski, E. M., et al. (2001). dbSNP: the NCBI database of genetic variation. *Nucleic Acids Res.* 29 (1), 308–311. doi:10.1093/NAR/29.1.308
- Shivakumar, D., Harder, E., Damm, W., Friesner, R. A., and Sherman, W. (2012). Improving the prediction of absolute solvation free energies using the next generation OPLS force field. *J. Chem. Theory Comput.* 8 (8), 2553–2558. doi:10.1021/ct300203w
- Stilgenbauer, S., Eichhorst, B., Schetelig, J., Hillmen, P., Seymour, J. F., Coutre, S., et al. (2018). Venetoclax for patients with chronic lymphocytic leukemia with 17p deletion: results from the full population of a phase II pivotal trial. *J. Clin. Oncol.* 36 (19), 1973–1980. doi:10.1200/JCO.2017.76.6840
- Szklarczyk, D., Gable, A. L., Nastou, K. C., Lyon, D., Kirsch, R., Pyysalo, S., et al. (2021). The STRING database in 2021: customizable protein–protein networks, and functional characterization of user-uploaded gene/measurement sets. *Nucleic Acids Res.* 49 (D1), D605–D612. doi:10.1093/nar/gkaa1074
- Tang, X., Wuest, M., Benesch, M. G. K., Dufour, J., Zhao, Y., Curtis, J. M., et al. (2020). Inhibition of autotaxin with GLPG1690 increases the efficacy of radiotherapy and chemotherapy in a mouse model of breast cancer. *Mol. Cancer Ther.* 19 (1), 63–74. doi:10.1158/1535-7163.MCT-19-0386
- Thomas, P. D., Ebert, D., Muruganujan, A., Mushayama, T., Albou, L. P., and Mi, H. (2022). PANTHER: making genome-scale phylogenetics accessible to all. *Protein Sci.* 31 (1), 8–22. doi:10.1002/pro.4218
- Vasileva, M. H., Bennemann, A., Zachmann, K., Schön, M. P., Frank, J., and Ulaganathan, V. K. (2024). CD24 flags anastasis in melanoma cells. *Apoptosis*, 1–15. doi:10.1007/S10495-024-01990-1/FIGURES/12
- Wang, J. Q., Li, J. Y., Teng, Q. X., Lei, Z. N., Ji, N., Cui, Q., et al. (2020). Venetoclax, a BCL-2 inhibitor, enhances the efficacy of chemotherapeutic agents in wild-type ABCG2-overexpression-mediated MDR cancer cells. *Cancers (Basel)* 12 (2), 466. doi:10.3390/CANCERS12020466
- Warde-Farley, D., Donaldson, S. L., Comes, O., Zuberi, K., Badrawi, R., Chao, P., et al. (2010). The GeneMANIA prediction server: biological network integration for gene prioritization and predicting gene function. *Nucleic Acids Res.* 38, W214–W220. doi:10.1093/NAR/GKQ537
- Xue, Y., Zhou, F., Zhu, M., Ahmed, K., Chen, G., and Yao, X. (2005). GPS: a comprehensive www server for phosphorylation sites prediction. *Nucleic Acids Res.* 33 (Web Server), W184–W187. doi:10.1093/nar/gki393
- Yalcin-Ozkat, G. (2021). Molecular modeling strategies of cancer multidrug resistance. *Drug Resist. Updat.* 59, 100789. doi:10.1016/j.drug.2021.100789
- Yin, X. M., Oltvai, Z. N., and Korsmeyer, S. J. (1994). BH1 and BH2 domains of Bcl-2 are required for inhibition of apoptosis and heterodimerization with Bax. *Nature* 369 (6478), 321–323. doi:10.1038/369321a0
- Youle, R. J., and Strasser, A. (2008). The BCL-2 protein family: opposing activities that mediate cell death. *Nat. Rev. Mol. Cell Biol.* 9 (1), 47–59. doi:10.1038/nrm2308
- Zaitceva, V., Kopeina, G. S., and Zhivotovsky, B. (2021). Anastasis: return journey from cell death. *Cancers.* 13 (15), 3671. doi:10.3390/CANCERS13153671